ELSEVIER

Catalysis Today 39 (1998) 343–350

CATALYSIS TODAY

Reversible structure change of one-atomic layer GeO_2 on SiO_2 surface under the interaction with Rh particles by in situ XAFS studies

Kazu Okumura[a], Kiyotaka Asakura[b], Yasuhiro Iwasawa[a,*]

[a]*Department of Chemistry, Graduate School of Science, The University of Tokyo, Hongo, Bunkyo-ku, Tokyo 113, Japan*
[b]*Research Center for Spectrochemistry, Faculty of Science, The University of Tokyo, Hongo, Bunkyo-ku, Tokyo 113, Japan*

Abstract

Structures of Rh/1 AL (atomic layer) GeO_2/SiO_2 were studied during reduction and oxidation processes by means of in situ XAFS (X-ray absorption fine structure). It was found that RhGe bimetallic particles with Rh–Rh and Rh–Ge distances at 0.266 and 0.242 nm were formed after reduction at 723 K, respectively. Subsequent oxidation at 673 K regenerated 1 AL GeO_2 structure on the SiO_2 surface. This reversible structure transformation is discussed in relation to reactivity and volatility of Ge oxide species. © 1998 Elsevier Science B.V.

Keywords: XAFS; Structural change; GeO_2 layer on SiO_2; Rh particles

---

1. Introduction

Catalytic properties of supported metals are not only determined by the kind of metals but also support materials through electronic or structural interactions with the supported metals. Thus the metal–support interaction is one of the important issues in the catalytic science. Many spectroscopic studies have been applied to reveal the mechanism of the metal–support interaction to get the structural and electronic information of the supported metal particles. However, we have few pieces of information about the structural change of support surface mediated by the metal–support interaction. TiO_2 is known as a strong metal–support interaction (SMSI) support, where partially reduced TiO_x suboxides migrate onto supported noble metal particles by high temperature reduction, which has been demonstrated by EXAFS, TEM and probe reactions [1–6]. However, local structure of the migrated Ti oxides is not clear because it is difficult to elucidate structural information of the migrated species from the spectra dominated by a large number of unchanged bulk TiO_2. When one-atomic layer (1 AL) structure of oxide is deposited on the surface of a high surface area support composed of a different element from the deposited one, it is possible to regard it as a model support surface and to investigate the change of surface layer selectively by means of EXAFS (extended X-ray absorption fine structure) due to its element specific character [7,8]. We have investigated the structure and surface behavior of 1 AL Nb_2O_5/SiO_2 and 1 AL TiO_2/SiO_2 prepared by a reactive CVD method [9–14]. Recently we have prepared SiO_2-supported one atomic layer GeO_2 material (denoted as 1 AL GeO_2/SiO_2 hereinafter) by the reaction of

---

[*] Corresponding author. Fax: +81 3 3814 2627; e-mail: iwasawa@chem.s.u-tokyo.ac.jp

0920-5861/98/$32.00
PII S0920-5861(97)00126-0

$Ge(OCH_3)_4$ with surface OH groups of SiO_2 [15]. GeO_2 has a hexagonal crystal structure which is the same as the structure of α-quarz. Niwa et al. [16,17] prepared GeO_2 layers on the outer surface of zeolites to modify the molecular sieving property of zeolites by using the similar preparation method. We have determined the structure of GeO_2/SiO_2 by EXAFS, IR, X-ray diffraction and X-ray fluorescence analysis. As a result, it was suggested that GeO_2 exists as one-atomic layer structure with Ge–O and Ge–Ge distances at 0.173 and 0.318 nm, respectively. Judging from the bond distances, the surface GeO_2 layer has a local structure similar to a hexagonal-type. In the present study this 1 AL GeO_2/SiO_2 was used as a support for Rh metal. The Rh/1 AL GeO_2/SiO_2 sample was prepared by interacting $[RhCH_3(C_5(CH_3)_5)]_2$-(μ-$CH_2)_2$ with the 1 AL GeO_2/SiO_2, followed by calcination with O_2 and by the reduction with H_2. Here we report structural analysis of Rh/1 AL GeO_2/SiO_2 by the oxidation and reduction treatments by EXAFS and XANES of Rh and Ge K-edges.

2. Experimental

2.1. Materials

$Ge(OCH_3)_4$ was purchased from Soekawa (purity=99.999%). Aerosil 300 was used as a SiO_2 support which was pretreated at 473 K for 1 h. $Ge(OCH_3)_4$ was deposited on the SiO_2 surface by chemical vapor deposition and the temperature was kept at 393 K for 1 h to complete the reaction with the surface OH groups. The unreacted $Ge(OCH_3)_4$ was evacuated at 473 K, followed by oxidation at 693 K for 1 h. The loading of Ge was determined to be 7.4 wt% by X-ray fluorescence. The loading corresponded to 1/5 ML assuming the two-dimensional GeO_2 unit cell area to be 0.1 nm^2. The further reaction of $Ge(OCH_3)_4$ with the OH groups of SiO_2 surface did not occur, which will be discussed elsewhere [15]. In this paper this surface was denoted as one-atomic layer (1 AL) GeO_2/SiO_2. The supported Rh catalysts were prepared by reaction of $[Rh(CH_3)(C_5(CH_3)_5]_2$-(μ-$CH_2)_2$ in $CHCl_3$ solution with the OH groups at room temperature under Ar atmosphere. $[Rh(CH_3)(C_5(CH_3)_5)]_2(\mu\text{-}CH_2)_2$ was synthesized according to the literature [18,19]. The solvent was evacuated under high vacuum at room temperature. The sample was then calcined at 673 K for 1 h. The loading of Rh was 2 wt%. The sample was treated in a U-shape tube combined with a closed circulating system. The oxidation of the sample was carried out by 21 kPa O_2 at 673 K and the reduction was performed with 13 kPa H_2 at 723 K. For comparison an SiO_2-supported Rh catalyst was prepared by using the Rh dimer in the same way as that for the 1 AL GeO_2/SiO_2 support.

2.2. EXAFS measurements

The treated samples were transferred without exposure to air to sample cells with two Kapton windows which were connected directly to the closed circulating system. The EXAFS measurement was carried out in Photon Factory in the National Laboratory for High Energy Physics (KEK-PF) (Proposal No. 94G203). The ring energy was 2.5 GeV with 250–350 mA. Rh K-edge EXAFS spectra were measured at BL-10B with a Si(3 1 1) channel cut monochromator. I_0 and I signals were detected by ionization chambers filled with Ar and Kr, respectively. Ge K-edge EXAFS data were collected at BL-7C where a sagittal focusing Si(1 1 1) double crystal monochromator is installed. The higher harmonics were eliminated by detuning the parallelism to 75% intensity of the maximum. I_0 and I monitors were filled with N_2 and Ar: N_2=25:75 mixed gas, respectively.

2.3. Data analysis

EXAFS data were analyzed using a program "REX". The background was removed by a cubic smoothing method, using Cook and Sayers criteria [20]. The extracted EXAFS oscillation was usually k^3-weighted and Fourier transformed to r-space over k=30–140 nm^{-1}. It was then inversely Fourier transformed again to k-space and curve fitting analysis was performed. Phase shift and amplitude functions for Rh–Rh, Ge–O and Ge–Ge were empirically derived from reference compounds, Rh foil, GeO_2 (hexagonal type) and Ge powder, respectively. The phase shift and amplitude functions for Rh–Ge and Ge–Rh were determined theoretically from FEFF program (Ver. 6) [21,22].

3. Results

3.1. EXAFS results on 1 AL GeO_2/SiO_2

Detailed structural analysis for the 1 AL GeO_2/SiO_2 will appear in a separate paper [15]. Here we will briefly describe its essence of structural results for convenience of the discussion on the Rh/1 AL GeO_2/SiO_2 catalyst. From X-ray diffraction, FT-IR spectra of the surface OH groups of GeO_2 and analysis by X-ray fluorescence, we concluded that the GeO_2 species are spread as a one-atomic layer structure on SiO_2 surface. Fig. 1 shows the k^3-weighted EXAFS oscillation, $k^3\chi(k)$ of the 1 AL GeO_2/SiO_2 and its Fourier transform. For comparison, the corresponding spectra of hexagonal GeO_2 bulk is depicted in Fig. 2. The peak height in the second shell corresponding to Ge–Ge bonding of the 1 AL GeO_2 is remarkably reduced compared to that for GeO_2. The bond lengths for Ge–O and Ge–Ge are determined to be 0.173 and 0.318 nm, respectively, by curve fitting analysis. Two types of crystal structure are known for the bulk GeO_2; the water-soluble hexagonal structure (Ge–O= 0.174 nm and Ge–Ge=0.315 nm) and the water-insoluble tetragonal one (Ge–O=0.187–0.190 nm and Ge–Ge=0.342 nm). The curve fitting results demonstrated that the structure of 1 AL GeO_2 is hexagonal-like. The 1 AL GeO_2/SiO_2 is stable against oxidation with O_2 at 673 K and reduction at 723 K though the layer structure is destroyed by exposure to water vapor to be converted to GeO_2 particles.

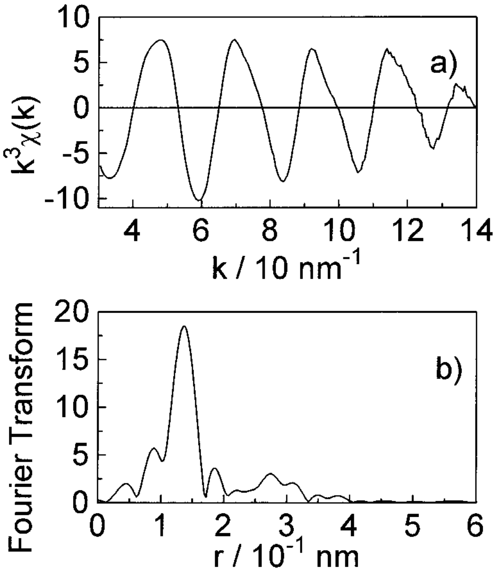

Fig. 1. Ge K-edge EXAFS data for 1 AL GeO_2/SiO_2; k^3-weighted EXAFS oscillation (a) and its Fourier transform (b).

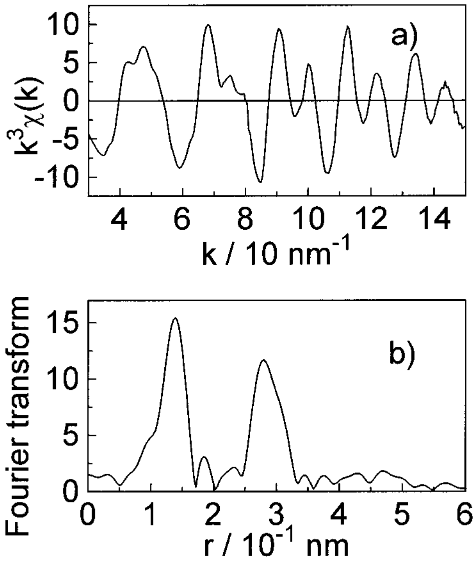

Fig. 2. Ge K-edge EXAFS data for GeO_2; k^3-weighted EXAFS oscillation (a) and its Fourier transform (b).

3.2. EXAFS results on Rh/1 AL GeO_2/SiO_2

Figs. 3 and 4 show the EXAFS oscillations at Ge and Rh K-edges for the Rh/1 AL GeO_2/SiO_2 reduced with H_2 at 723 K and its Fourier transform, respectively. The EXAFS oscillations for 1 AL GeO_2/SiO_2 were changed by Rh deposition. To clarify the difference in the spectra we subtracted the k^3-weighted EXAFS oscillation of Fig. 1 from that of Fig. 3. The difference spectra were affected by the procedures of measurements and data analyses. Therefore we used two spectra of 1 AL GeO_2/SiO_2 and Rh/1 AL GeO_2/SiO_2 at the same experimental run. We used the cells with the same thickness and carefully prepared two samples with almost the similar absorbance. The same background removal processes, k-weights, and normalization points were applied to obtain the EXAFS oscillations for two spectra. The calculation of difference spectra was carried out as follows: the

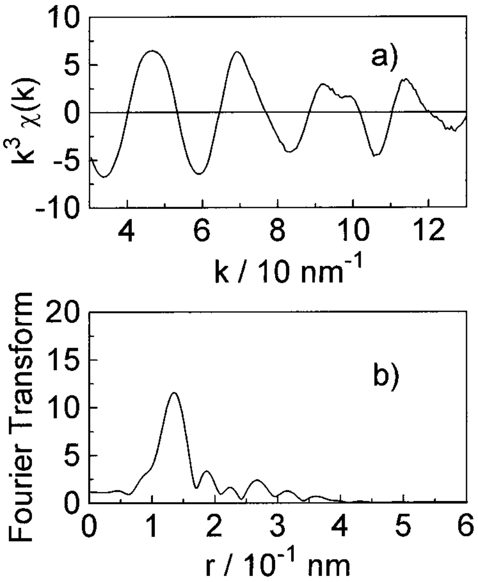

Fig. 3. Ge K-edge EXAFS data for Rh/1 AL GeO_2/SiO_2 reduced at 723 K; k^3-weighted EXAFS oscillation (a) and its Fourier transform (b).

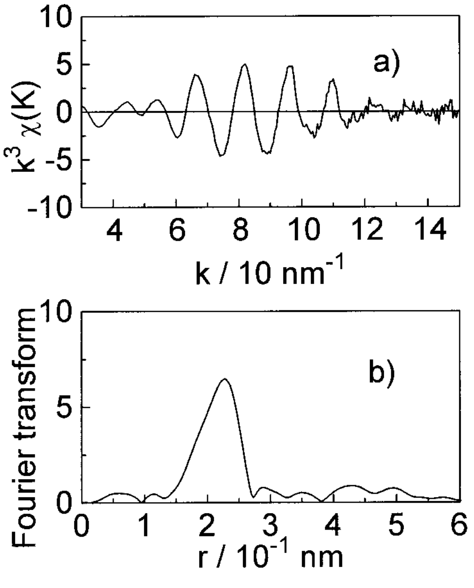

Fig. 4. Rh K-edge EXAFS data for Rh/1 AL GeO_2/SiO_2 reduced at 723 K; k^3-weighted EXAFS oscillation (a) and its Fourier transform (b).

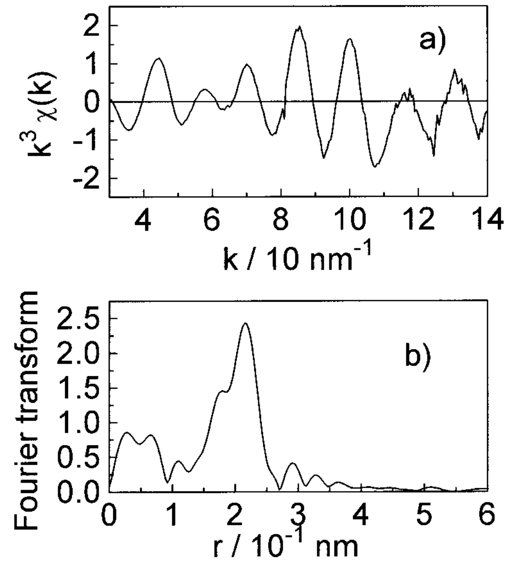

Fig. 5. (a) Difference $k^3\chi(k)$ between Rh/1 AL GeO_2/SiO_2 reduced at 723 K in Fig. 3 and 1 AL GeO_2/SiO_2 in Fig. 1, (b) its associated Fourier transform.

$\chi(k)$ of 1 AL GeO_2/SiO_2. The resulting spectrum was assumed to correspond to the GeO_2 species for Rh/1 AL GeO_2/SiO_2 reduced at 723 K. Fig. 5 depicted the difference spectrum of $k^3\chi(k)$ and its Fourier transform. A peak appeared at 0.21 nm. We checked the effects of the k-weights, normalization points and different background removal method such as cubic spline method and we always found the peak around 0.21 nm. The peak at 0.21 nm is longer than Ge–O and much shorter than Ge–Ge in GeO_2. There are two possibilities for the origin of this peak; one is Ge–Ge and the other is Ge–Rh with direct bonding produced after high temperature reduction. The better fitting result was obtained when Ge–Rh boning was assumed at 0.240 nm with 0.5 of the coordination number as shown in Fig. 6 indicating the formation of bimetallic cluster.

The Rh K-edge EXAFS oscillation and its Fourier transform over 30–150 nm^{-1} for the reduced Rh/1 AL GeO_2/SiO_2 in Fig. 4 were also different from those for Rh/SiO_2 in Fig. 7. The difference in the Rh K-edge EXAFS between Rh/1 AL GeO_2/SiO_2 and Rh/SiO_2 is observed not only in peak height but also in peak position which appears in a shorter bond length for that of Rh/1 AL GeO_2/SiO_2. The shortening of bond length occurred probably due to the formation of the direct Rh–Ge bonding. We carried out curve fitting analysis for the inversely Fourier transformed data over 0.15–0.30 nm. When the peak was assumed to be

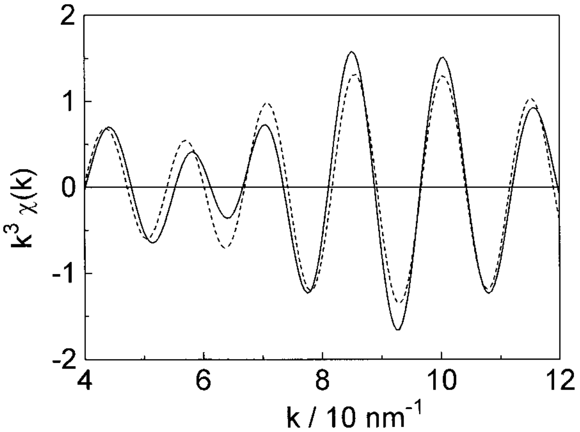

Fig. 6. Curve fitting for the inversely Fourier transformed data of Fig. 5(b) over 0.15–0.28 nm assuming Ge–Rh bonding.

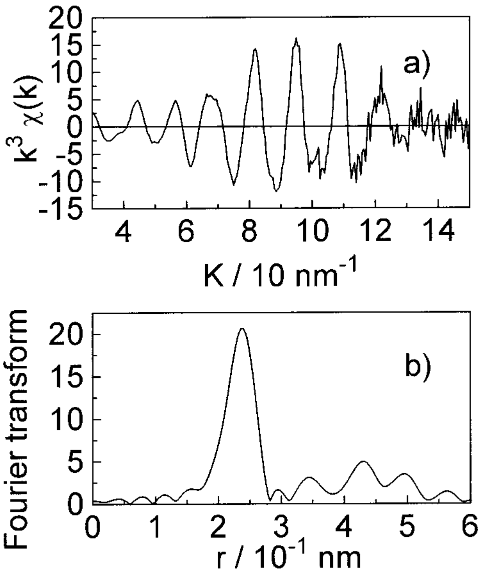

Fig. 7. k^3-weighted Rh K-edge EXAFS oscillation (a) of Rh/SiO$_2$ and its Fourier transform (b).

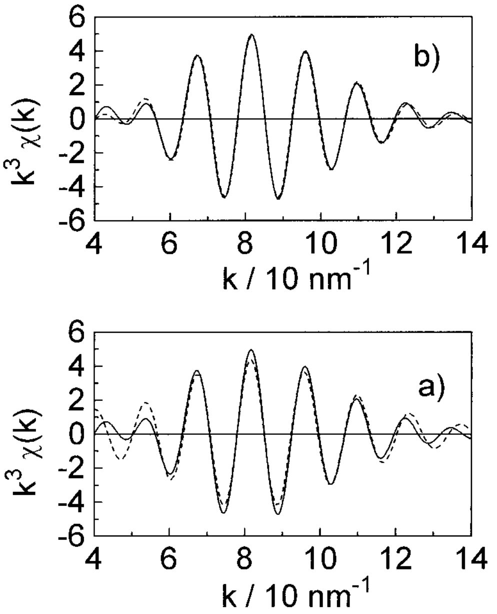

Fig. 8. Fitting results of the inversely Fourier transformed data over 0.15–0.30 nm of Rh/1 AL GeO$_2$/SiO$_2$ assuming one wave Rh–Rh bonding (a) and two waves (Rh–Rh+Rh–Ge) (b).

composed of one Rh–Rh contribution, the calculated curve did not sufficiently reproduce the observed data well as shown in Fig. 8(a) and in Table 1. When we added a Rh–Ge direct bonding at 0.242 nm, we successfully reproduced the observed EXAFS oscillation as shown in Fig. 8(b) and also in Table 1. This result agrees with the Ge K-edge EXAFS observation which also indicates the presence of Ge–Rh at 0.240 nm. Thus after the reduction of Rh/1 AL GeO$_2$/SiO$_2$ at 723 K, the 1 AL GeO$_2$ is suggested to be partially reduced to form RhGe bimetallic particles.

X-ray absorption near edge structure gives more information about the valence state of the X-ray

Table 1
Curve fitting results for Rh/1 AL GeO$_2$/SiO$_2$

Model	Atomic pair	*N*	*r* (nm)	E_0 (eV)	σ^2 (nm^2)	*R* (%)[a]
(a)	Rh–Rh	6.3	0.261	−23	7.2×10^{-5}	12
(b)	Rh–Rh	3.7	0.266	−12	5.6×10^{-5}	2.2
	Rh–Ge	1.4	0.242	−10	5.0×10^{-5}	

[a] Residuals for the curve fitting defined as $\sqrt{N_{\mathrm{pts}}/(N_{\mathrm{pts}}-p)(1/N)\Sigma(\chi_{\mathrm{obs}}-\chi_{\mathrm{cal}})^2/\Sigma\chi^2_{\mathrm{cal}}}$, where N_{pts} is the number of freedom for independent fitting parameters calculated by $2\Delta k\Delta r/\pi = 2\cdot120\cdot0.15/\pi \approx 10$, and p is the number of fitting parameters.

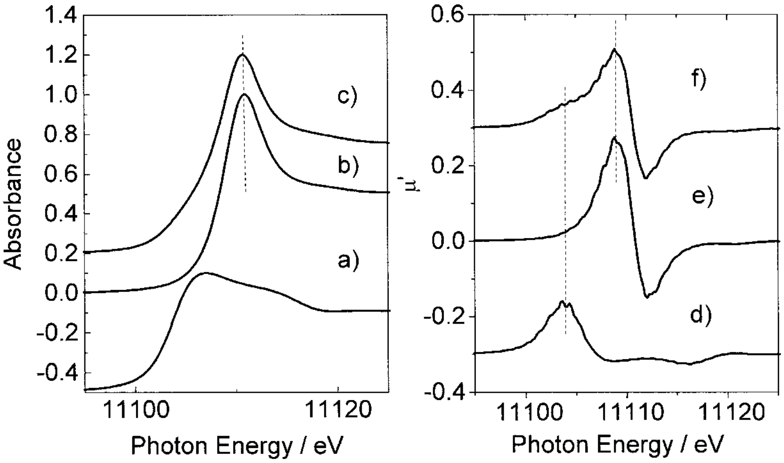

Fig. 9. XANES spectra and their first derivatives, $d\mu/dE$, of Ge K-edges for Ge ((a) and (d)), 1 AL GeO_2/SiO_2 ((b) and (e)), and Rh/1 AL GeO_2/SiO_2 reduced at 723 K ((c) and (f)), respectively.

absorbing atom. Fig. 9 shows the Ge K-edge XANES spectra of 1 AL GeO_2/SiO_2 and Rh/1 AL GeO_2/SiO_2 reduced at 723 K as well as Ge powder. Although the position of edge peak does not change after the deposition of Rh and the reduction at 723 K, a small shoulder appears around 11 107 eV in the Rh/1 AL GeO_2/SiO_2 sample reduced at 723 K. To see more clearly the peak position, we differentiated the spectra by photon energy as shown in the right frame ((d)–(f)) of Fig. 9. The shoulder structure appears at 11 103 eV in the first derivative of the XANES spectrum of Rh/1 AL GeO_2/SiO_2 which may correspond to the peak in that of Ge powder. These results reflect the presence of the Ge species with much lower oxidation states than 4+ (probably nearly 0) in the Rh/1 AL GeO_2/SiO_2. Thus the XANES studies also confirm that the Ge species in the Rh/1 AL GeO_2/SiO_2 is also reduced after the reduction at 723 K.

On the other hand no reduction occurred for 1 AL GeO_2/SiO_2 without Rh supported on it from XANES and EXAFS results. The reduction of GeO_2 may happen by the spillover hydrogen from the Rh metal particles in the neighborhood of the Rh particles.

3.3. *Structure of 1 AL* GeO_2 *in Rh/1 AL* GeO_2/SiO_2 *after reoxidation*

The RhGe particles formed on 1 AL GeO_2/SiO_2 after reduction at 723 K were oxidized with O_2 at 673 K to Rh oxide (denoted as RhO_x) and GeO_2. Interestingly, no X-ray diffraction pattern attributable to GeO_2 particles was seen. Therefore we measured Ge K-edge EXAFS of the Rh/1 AL GeO_2/SiO_2 sample reoxidized at 673 K. Fig. 10 shows the k^3-weighted EXAFS oscillation and its Fourier transform. Compared with Figs. 1 and 3, it is concluded that the GeRh

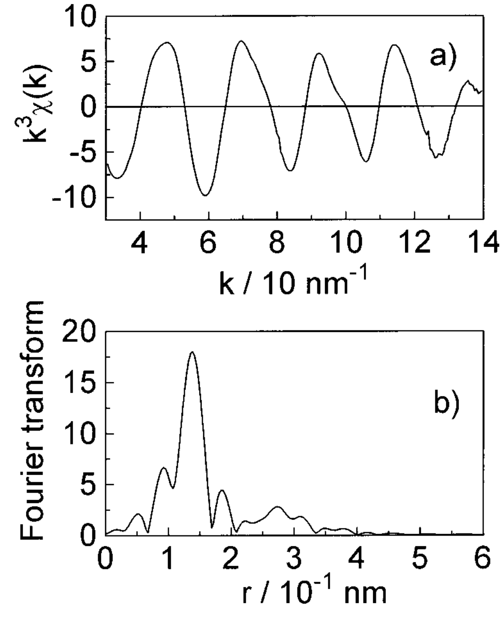

Fig. 10. Ge K-edge EXAFS data for Rh/1 AL GeO_2/SiO_2 reoxidized with O_2 at 673 K; the k^3-weighted EXAFS oscillation (a) and its Fourier transform (b).

bimetallic particles were destroyed to form the GeO_2 species identical to the 1 AL GeO_2/SiO_2. No increase in Ge–Ge peak intensity in Fig. 10(b) indicates the regeneration of the original 1 AL GeO_2/SiO_2 structure without aggregation to the GeO_2 bulk particle. The regeneration of the one-atomic layer structure after reoxidation was also supported by IR observation of surface OH groups on GeO_2. The intensity of ν(OH) peaks did not change between the original calcined Rh/1 AL GeO_2/SiO_2 sample before reduction and the reoxidized sample after the reduction treatment.

4. Discussion

The 1 AL GeO_2/SiO_2 was not reduced by H_2 at 773 K. However, in the presence of Rh the reduction of the 1 AL GeO_2 occurred probably due to the spillover hydrogen from the reduced Rh particles on the 1 AL GeO_2/SiO_2. As a result of reduction, Rh–Ge bimetallic particles were formed as shown by the curve fitting analyses of both Ge K-edge and Rh K-edge for Rh/1 AL GeO_2/SiO_2 and also by XANES spectra. The Rh–Ge distances are 0.241±0.003 nm (averaged values determined from Rh K-edge EXAFS and Ge K-edge EXAFS). This value is shorter than the value 0.257 nm estimated from the sum of the bond lengths of the elements, i.e., Ge–Ge in Ge and Rh–Rh in Rh metal are 0.24498 and 0.26901 nm, respectively. This fact indicates that the Rh–Ge bonding has a covalent character than a metallic one. Furthermore, it is interesting that Rh–Rh bond length 0.266±0.003 nm in the RhGe bimetallic system is similar to the Rh–Rh bonding in the Rh foil and not so affected by the Rh–Ge bonding. This probably means that the RhGe bimetal does not form solid solution structure but causes segregation of Ge at the surface of the bimetallic particles. As the particle size of RhGe bimetallic species has not been measured by transmission electron microscope, we do not know the exact reason why the Fourier transform peak in Fig. 4 is much smaller than that of the corresponding Rh/SiO_2. It may be referred to small particle size due to the interaction of Ge–Rh bonding.

It was found that the RhGe bimetallic system had no chemisorption ability for H_2. The phenomenon is similar to the SMSI effect. In SMSI catalysts like Pt/TiO_2 and Rh/TiO_2, the partially reduced TiO_x suboxides formed by high-temperature H_2 reduction migrates onto the Pt or Rh particles, which blocks the adsorption of H_2 and CO [2,5,6]. In Rh/TiO_2 the direct Rh–Ti bond formation was reported where Rh–Ti bond length was 0.253 nm [6] though there is still debate. The present study on the 1 AL GeO_2 more clearly demonstrates the presence of direct Rh–Ge bonding in the reduced sample. Thus GeO_2 can also be classified as SMSI support.

The reoxidation of the sample destroyed the RhGe bimetallic structure. The results of EXAFS, X-ray diffraction and FT-IR spectra of the surface OH groups indicated that the 1 AL GeO_2 was reproduced on the SiO_2 surface and three-dimensional GeO_2 particles were not formed. The structural changes during the reduction and oxidation are summarized in Fig. 11. This structure change is unique. Bulk GeO_2 particle is more stable than the 1 AL GeO_2 species on SiO_2, because the 1 AL GeO_2 species was only formed by the reaction of $Ge(OCH_3)_4$ and surface OH groups of SiO_2 and is never produced by the solid state reaction between GeO_2 and SiO_2 at high temperatures. In fact, once three-dimensional GeO_2 particles were produced from the 1 AL GeO_2 by the interaction with H_2O vapor, they were stable with any treatment and not converted to 1 Al GeO_2. The state of 1 AL GeO_2 may be thermodynamically metastable state. When the RhGe bimetallic particles were oxidized with O_2 at 673 K, the oxygen intrudes into Ge–Rh bonding and Ge–O and Rh–O were formed. If the further oxidation occurred, bulk GeO_2 particles would have been pro-

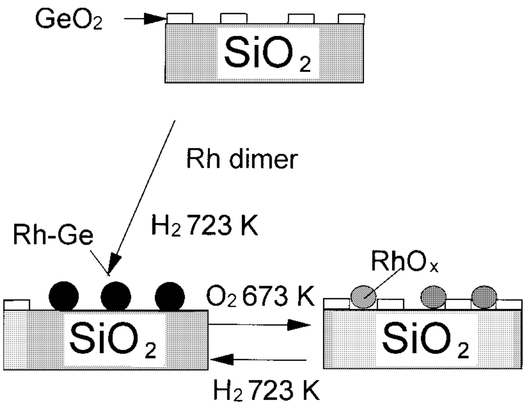

Fig. 11. A scheme for surface structure change of the Rh/1 AL GeO_2/SiO_2 by reduction and reoxidation.

duced. Considering that GeO is volatile species (sublimation temperature 983 K), we propose the following mechanism. First Ge(2+)–O is created in the RhGe bimetallic particles, then Ge(2+)-oxide molecules or clusters would be migrated or sublimed onto high surface-area SiO_2 surface. Finally the GeO species are transformed to the hexagonal-type GeO_2 layer on the SiO_2 surface. Because the surface area of the SiO_2 is quite high, formation of three-dimensional GeO_2 particles are kinetically suppressed even if they are thermodynamically stable. We are now proceeding further experiments in order to prove the above mechanism for a reversible transformation of the 1 AL GeO_2/SiO_2 and the RhGe bimetallic phase by means of other spectroscopic techniques.

References

[1] S.J. Tauster, S.C. Fung, R.T.K. Baker, J.A. Horsley, Science 211 (1981) 1121.
[2] D.E. Resasco, G.L. Haller, J. Catal. 82 (1983) 279.
[3] A. Singh, P.N.K. Bell, A.T. Bell, J. Catal. 94 (1985) 422.
[4] T. Yokoyama, K. Asakura, Y. Iwasawa, H. Kuroda, J. Phys. Chem. 93 (1989) 8323.
[5] D.E. Resasco, R.S. Weber, S. Sakellson, M. McMillan, G.L. Haller, J. Phys. Chem. 92 (1988) 189.
[6] S. Sakellson, M. McMillan, G.L. Haller, J. Phys. Chem. 90 (1986) 1733.
[7] D.C. Koningsberger, R. Prins (Eds.), X-ray Absorption, Principles, Applications, Techniques of EXAFS, SEXAFS, and XANES, Wiley, New York, 1988.
[8] Y. Iwasawa (Ed.), X-ray Absorption Fine Structure for Catalysts and Surfaces, World Scientific, Singapore, 1996.
[9] K. Asakura, J. Inukai, Y. Iwasawa, J. Phys. Chem. 96 (1992) 829.
[10] K. Asakura, Y. Iwasawa, J. Phys. Chem. 95 (1991) 1711.
[11] K. Asakura, Y. Iwasawa, Chem. Lett. (1988) 633.
[12] K. Asakura, Y. Iwasawa, Chem. Lett. (1986) 859.
[13] M. Shirai, N. Ichikuni, K. Asakura, Y. Iwasawa, Catal. Today 8 (1990) 57.
[14] M. Shirai, K. Asakura, Y. Iwasawa, J. Phys. Chem. 95 (1991) 9999.
[15] K. Okumura, K. Asakura, Y. Iwasawa, to be published.
[16] M. Niwa, S. Kato, T. Hattori, Y. Murakami, J. Chem. Soc., Faraday. Trans. I 80 (1984) 3135.
[17] M. Niwa, M. Kato, T. Hattori, Y. Murakami, J. Phys. Chem. 90 (1986) 6233.
[18] K. Isobe, A. Vazwuez de Miguel, P.M. Bailey, S. Okeya, P.M. Maitlis, J. Chem. Soc., Dalton Trans. (1983) 1441.
[19] K. Isobe, D.G. Andrews, B.E. Mann, P.M. Maitlis, J. Chem. Soc. Chem. Commun. (1981) 809.
[20] J.W. Cook, D.E. Sayers, J. Appl. Phys. 52 (1981) 5024.
[21] J.J. Rehr, R.C. Albers, S.I. Zabinsky, Phys. Rev. Lett. 69 (1992) 3418.
[22] J.J. Rehr, J. Mustre de Leon, S.I. Zabinsky, R.C. Albers, J. Am. Chem. Soc. 113 (1991) 5135.